



HAL
open science

Shading devices optimization to enhance thermal comfort and energy performance of a residential building in Morocco

Haitham Sghiouri, Ahmed Mezrhab, Mustapha Karkri, Hassane Naji

► **To cite this version:**

Haitham Sghiouri, Ahmed Mezrhab, Mustapha Karkri, Hassane Naji. Shading devices optimization to enhance thermal comfort and energy performance of a residential building in Morocco. *Journal of Building Engineering*, 2018, 18, pp.292-302. 10.1016/j.job.2018.03.018 . hal-04315324

HAL Id: hal-04315324

<https://hal.u-pec.fr/hal-04315324v1>

Submitted on 24 Apr 2024

HAL is a multi-disciplinary open access archive for the deposit and dissemination of scientific research documents, whether they are published or not. The documents may come from teaching and research institutions in France or abroad, or from public or private research centers.

L'archive ouverte pluridisciplinaire **HAL**, est destinée au dépôt et à la diffusion de documents scientifiques de niveau recherche, publiés ou non, émanant des établissements d'enseignement et de recherche français ou étrangers, des laboratoires publics ou privés.

Author's Accepted Manuscript

Shading devices optimization to enhance thermal comfort and energy performance of a residential building in Morocco

Haitham Sghiouri, Ahmed Mezrhab, Mustapha Karkri, Hassane Naji



PII: S2352-7102(17)30660-5
DOI: <https://doi.org/10.1016/j.job.2018.03.018>
Reference: JOBE440

To appear in: *Journal of Building Engineering*

Received date: 26 October 2017
Revised date: 18 March 2018
Accepted date: 22 March 2018

Cite this article as: Haitham Sghiouri, Ahmed Mezrhab, Mustapha Karkri and Hassane Naji, Shading devices optimization to enhance thermal comfort and energy performance of a residential building in Morocco, *Journal of Building Engineering*, <https://doi.org/10.1016/j.job.2018.03.018>

This is a PDF file of an unedited manuscript that has been accepted for publication. As a service to our customers we are providing this early version of the manuscript. The manuscript will undergo copyediting, typesetting, and review of the resulting galley proof before it is published in its final citable form. Please note that during the production process errors may be discovered which could affect the content, and all legal disclaimers that apply to the journal pertain.

Shading devices optimization to enhance thermal comfort and energy performance of a residential building in Morocco

Haitham Sghiouri^a, Ahmed Mezrhab^{a*}, Mustapha Karkri^b, Hassane Naji^{c,d}

^aUniversité Mohamed Premier, Mechanics and Energetic Laboratory, 60000, Oujda, Morocco.

^bUniversité Paris-Est, CERTES, 61 Avenue du Général de Gaulle, 94010 Créteil Cedex, France

^cUniv. Artois, Civil Engineering and Geo-Environment Laboratory (LGCgE - EA 4515), F-62400 Béthune, France.

^dLille University Northern France, LGCgE - EA 4515, F-59000 Lille, France.

*Corresponding author. amezrhab@yahoo.fr (A. Mezrhab)

ABSTRACT

Morocco's building sector accounts for about 25% of the country's total energy consumption, including 18% for residential and 7% for the services sector. This energy consumption is expected to raise due to the significant rise of household equipment rate in HVAC facilities mainly air-conditioners. This work presents a methodology combining single-objective optimization and building energy simulation, applied to the study of the effect of optimized overhangs, aimed at improving thermal comfort of a typical two-storey Moroccan existing building in three different climates of Marrakech, Casablanca and Oujda. The optimization has been performed using the non-dominated sorting genetic algorithm (NSGA-II). Optimal and benchmark cases are compared regarding the percentage of annual discomfort, cooling demand and heating demand. The results show that the thermal comfort is improved, and the optimized overhangs reduce the cooling demand by 4.1% for Casablanca's mediterranean climate, which exhibits no contradiction between improvements in thermal comfort and performance.

Keywords:

Building; genetic algorithm; optimization; adaptive thermal comfort; shading; TRNSYS.

Nomenclature

Depth Depth below surface [m]

DDH_{mean} Area-weighted discomfort degree-hours [$^{\circ}\text{C}\cdot\text{h}$]

dH Degree-hours [$^{\circ}\text{C}\cdot\text{h}$]

DH_{Zx} Discomfort degree-hours in thermal zone x [$^{\circ}\text{C}\cdot\text{h}$]

$f_i(\mathbf{X})$ Objective function

$\mathbf{F}(\mathbf{X})$ Vector of objective functions

$g_m(\mathbf{X})$ Inequality constraint

$\mathbf{G}(\mathbf{X})$ Vector of inequality constraints

g-value Solar heat gain coefficient

$h_n(\mathbf{X})$ Equality constraint

$\mathbf{H}(\mathbf{X})$ Vector of equality constraints

h_{inside} Heat transfer coefficient of internal surfaces [$\text{W}\cdot\text{m}^{-2}\cdot\text{K}^{-1}$]

h_{outside} Heat transfer coefficient of external surfaces [$\text{W}\cdot\text{m}^{-2}\cdot\text{K}^{-1}$]

t_{now} Current day of the year [day]

t_{shift} Day of the year corresponding to the minimum surface temperature [day]

T Soil temperature at a specified depth [$^{\circ}\text{C}$]

T_{air} Air temperature inside the considered thermal zone [$^{\circ}\text{C}$]

T_{amp} Amplitude of surface temperature [$^{\circ}\text{C}$]

T_c Comfort temperature [$^{\circ}\text{C}$]

$T_{\text{ed-x}}$ Mean external temperature at the x day before the current day [$^{\circ}\text{C}$]

T_{mean} Mean surface temperature [$^{\circ}\text{C}$]

T_{op} Operative temperature [$^{\circ}\text{C}$]

T_{rm}	External running mean temperature [$^{\circ}\text{C}$]
T_{surf}	Inside surface temperature [$^{\circ}\text{C}$]
U_{value}	Thermal transmittance of the glazing area [$\text{W}/\text{m}^2.\text{K}$]
V	Wind speed [$\text{m}.\text{s}^{-1}$]
X	Vector of problem variables
x_k	Overhang projection [m]
α	Thermal diffusivity of the ground (soil) [$\text{m}^2.\text{day}^{-1}$]

Acronyms

AMEE Agence Marocaine pour l'Efficacité Energétique

ASHRAE American Society of Heating, Refrigerating and Air-conditioning Engineers

CSTB Centre Scientifique et Technique du Bâtiment

DDH Discomfort degree-hours

GHI Global horizontal irradiance

GND Ground

HVAC Heating, ventilating, and air conditioning

RTCM Règlement Thermique de Construction au Maroc

TMY Typical Meteorological Year

WWR Window-to-Wall Ratio

1 Introduction

Buildings energy consumption in Morocco ranks second, after the transport sector, with a 25% share of total energy consumption in the country, of which 18% for residential and 7% for the services sector [1]. Furthermore, energy consumption is expected to rise rapidly in the upcoming years for two main reasons:

- A significant rise in household equipment rate in HVAC facilities due to their affordable prices and the improvement of Moroccans living standards;
- A rapidly growing building sector in the country.

The equipment rate in heating devices of residential housing increased from 1.9% in 2000 to 4.9% in 2010, thanks to widespread use of electricity in rural areas and improved living standards. Thereby, energy consumption, for heating, has almost doubled from 300 MWh to 581 MWh. Besides, the equipment rate in air-conditioning devices follows the same pattern, as it tripled from 3% to 10% between 2000 and 2010. To reduce this demand for cooling, the use of external shading devices is one of the most effective strategies especially in hot climates, since it protects the building from solar radiation before reaching the glazed area in summer conditions. Thus, it avoids overheating by decreasing unwanted heat gains through fenestrations.

In the literature, there are many studies on the role of shading devices in improving the comfort of occupants and thermal performance of buildings. Yun et al. [2] evaluated visual comfort and building energy demand, and suggested lighting and shading control strategies to improve visual comfort and energy savings of office buildings. Kim et al. [3] proposed an experimental configuration of an external shading device for apartment houses in South Korea. It was then compared to conventional daylighting devices in terms of energy savings through simulations made in IES Virtual Environment. The experimental shading device showed the most efficient performance and also provides better views for occupants. Bellia et al. [4] studied the influence of external solar shading devices on the energy requirements of a typical air-conditioned office building for Italian climates by the mean of a dynamic simulation using EnergyPlus. Samani et al. [5] investigated four passive cooling techniques for a pre-fabricated building, namely, exterior shading, natural ventilation, increase of interior gypsum plaster thickness and cool painting, by comparing their impact on average indoor air

and thermal comfort of occupants based on ASHRAE 55 and EN 15251 standards. The study demonstrated the superiority of natural ventilation and exterior shading followed by cool painting and increase in thickness of gypsum plaster for decreasing high temperatures.

Ebrahimipour et al. [6] investigated the effect of Low-E glazing and overhangs on the solar energy transmitted into or lost from the room through the fenestration areas for typical residential buildings in Tehran, by the mean of EnergyPlus simulation software. Aldawoud [7] compared the performance and the effectiveness of electrochromic glazing system to conventional fixed shading device in hot, dry climate for a typical office building modelled in DesignBuilder. It was found that electrochromic glazing system shows the best performance in reducing solar heat gains.

Many researchers worked on semitransparent shadings such as Olivieri et al. [8] who analyzed the energy performance of five STPV (semi-transparent photovoltaic) elements, using the following simulation tools: DesignBuilder, EnergyPlus, PVsyst, and COMFEN, it was found that STPV elements provide between 18% and 59% of energy saving potential compared to reference glass. Cornaro et al. [9] assessed the energy saving potential of four different types of STPV (Dye sensitized solar modules and thin film modules) compared to conventional double pane glass. Simulations of different orientations of an office building at three different locations in Italy (Rome, Trento and Palermo) were performed using IDA ICE. It was found that Dye sensitized solar modules have the best performance. Frasca et al. [10] worked on the retrofit of a prefabricated building in order to reduce the excess in summer heat using PV system and static shadings which were optimized involving the tilt angle and the distance of the PV arrays. The results show that the proposed design achieves a decrease of 0.5°C in the maximum daily fluctuation and a reduction of 0.4°C of yearly mean temperature compared to the building without retrofit.

Regarding multi-objective optimization, Penna et al. [11] investigated the effect of the initial characteristics of residential buildings on the definition of optimal retrofit solutions considering economy, comfort and energy performance by the mean of a multi-objective optimization that has been performed using a genetic algorithm (NSGA-II) coupled with a dynamic simulation tool (TRNSYS). The results show that the cost-optimal solutions lead to more than 57% of energy saving but at the cost of worsening the thermal comfort. The study does not take into account the management of the shadings closing nor windows opening by occupants. Asadi et al. [12] presented a model combining a multi-objective optimization and artificial neural network (ANN) to assess technology choices in a school building. The multi-objective optimization algorithm is a variant of NSGA-II. The use of ANN helped to reduce the calculation time to 3 days instead of 75 days that would have been necessary in the case of using an exhaustive-computation search method. A single-objective optimization is conducted in order to understand the impact of each set of objective function and retrofit actions on the building's performance after retrofit focusing on building's energy consumption, retrofit cost, and thermal discomfort hours. Followed by a multi-objective optimization conducted in order to study the interaction between these three conflicting objectives. Magnier et al. [13] described an optimization methodology based on a combination of an Artificial Neural Network (ANN) and a multi-objective evolutionary algorithm. After the training of the ANN on 450 training cases, the ANN was implemented inside NSGA-II multi-objective optimization algorithm in order to get fast evaluations. Regarding results of the optimizations, reduction of the energy consumption as well as improvement in thermal comfort of the house has been shown. Hamdy et al. [14] proposed a modified multi-objective optimization approach based on GA (Genetic Algorithm) coupled with a building performance simulation program (IDA ICE). The approach is then used to minimize the carbon dioxide equivalent (CO₂-eq) emissions and the investment cost for three studied cases with different thermal

overheating levels focusing on heat recovery type, heating/cooling energy source, and six building envelope parameters as design variables. The study concludes that this approach can be used in the design phase to give a better understanding of the performance of the building and its HVAC systems. Roberti et al. [15] presented a combination between an analytic hierarchy process (AHP), a dynamic simulation and a multi-objective optimization to define a set of good retrofits for a historical building. Delgarm et al. [16] presented a novel approach for simulation-based optimization of buildings energy consumption using NSGA-II algorithm. EnergyPlus was used to perform the building energy simulation, while jEPlus was used as an interface between EnergyPlus and MATLAB where the optimization algorithm was used to obtain optimal values for the building orientation, the window size, and overhang specifications. Futrell et al. [17] performed a complex optimization of a classroom design using both pattern search and meta-heuristic optimization to optimize thermal performance and lighting demand. Chen et al. [18] conducted a variance-based sensitivity analysis to reduce search space, followed by a multi-objective optimization with NSGA-II algorithm using jEPlus and EnergyPlus to minimize lighting and cooling energy demand for a typical architectural form. Tian et al. [19] performed both a review and a comparison of existing techniques and optimization tools, viz., BEopt [20], jEPlus+EA [21], MOBO [22], DesignBuilder, GENE_ARCH [23], and MultiOpt [24].

As far as we know, only jEplus+EA, MOBO, Genopt [25], MultiOpt and TRNOPT can be coupled with TRNSYS. Therefore, we chose to use jEplus+EA for its parallel computing aptitudes. Note that MOBO does not have enough support (documentation) to couple it with TRNSYS. As for MultiOpt, it is not a freeware and is no longer distributed by the CSTB (Table 1).

Table 1 Comparison of some existing energy optimization tools for TRNSYS.

	jEplus+EA	GenOpt	MOBO	MultiOpt	TRNOPT
<i>Freeware</i>	Yes	Yes	Yes	No	No
<i>Parallel computing</i>	Yes	Yes	Yes	?	No
<i>Multi-objective</i>	Yes	No	Yes	Yes	No

These studies have highlighted the usefulness of shading devices in energy saving and comfort and have provided several ideas as to their optimization. Therefore, it is interesting to study the shading devices' impact on the thermal comfort and cooling demand of a typical Moroccan building, given that this technique is not extensively used.

The main focus of this paper is to present a methodology combining genetic algorithm (GA) through jEPlus and building energy simulation (TRNSYS) to improve the summer comfort of the occupants of a typical existing building for three different climates in Morocco using optimized overhangs.

In the following sections, the simulation methodology for a typical Moroccan building used in the analysis is described. Next, the results achieved for three different climates in Morocco are presented and commented on. Finally, the main conclusions of the work are summarized.

2 Methodology

2.1 Optimization

jEPlus is an open source tool initially developed to handle complex parametric simulations using EnergyPlus (E+) [26]. Combined with optimization algorithms such as genetic algorithms, it provides an efficient approach to perform optimization for building design and operation.

The NSGA-II is the base algorithm used in jEPlus+EA. It was customized to use integer encoding, hybrid crossover and mutation operators, and Pareto archiving methods [21]. In this study, the optimization algorithm was configured as described in Table 2.

Table 2 Optimization algorithm.

Algorithm	NSGA-II
Maximum population size	150
Population size	8
Crossover rate	1
Mutation rate	0.2
Tournament selection size	2

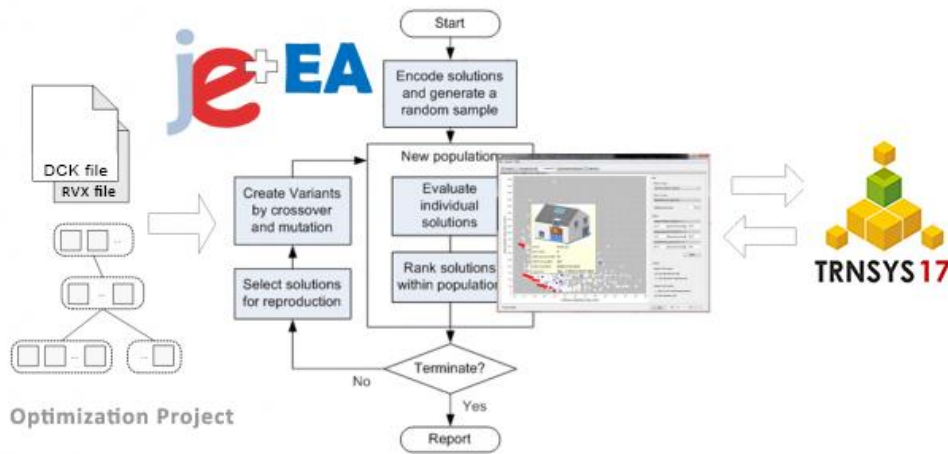


Fig. 1. Optimization project.

As described in Fig.1, the DCK file is generated by TRNSYS and contains all the information needed to perform the simulation, jEPlus imports the DCK and all files that are called in the DCK file in a same folder to start the simulation. The RVX file gathers a summary of the user-defined variables that will be plotted in jEPlus, as well as the constraints and objectives needed to execute the optimization. To perform this optimization, more information is collected from the TRNSYS simulation and stored in a file called totals.csv,

which is then used by jEPlus to perform the optimization, the data stored in totals.csv are the following:

- Discomfort degree-hours for each zone which are used to define the objective function.
- Heating/cooling energy demand of airnode as a result of the simulation.
- Discomfort hours as a result of the simulation.

2.2 Objective function

An optimization problem is generally expressed as follows:

$$\begin{aligned} \text{Minimize: } & J = F(X) \\ \text{Subject to: } & G(X) \leq 0 \\ & H(X) = 0 \end{aligned} \quad (1)$$

Where $X = [x_1, x_2, \dots, x_k]$ is the vector of problem variables;

$F(X) = [f_1(X), f_2(X), \dots, f_l(X)]$ is the vector of objective functions;

$G(X) = [g_1(X), g_2(X), \dots, g_m(X)]$ is the vector of inequality constraints;

$H(X) = [h_1(X), h_2(X), \dots, h_n(X)]$ is the vector of equality constraints.

Note that in this study, it's about a single-objective non-constrained optimization, so only one objective function is defined and no constraints are used.

jEPlus is coupled with TRNSYS to perform a single-objective optimization, aiming to minimize the discomfort degree-hours by modifying the overhangs projections in four different thermal zones of the building, where a unique optimal solution is found after the end of the 150 generations. The adaptive comfort model described below is used to get the temperatures above and beneath which occupants feel discomfort in summer conditions, those temperatures are used to calculate the discomfort degree-hours, as for the rest of the year, constant temperatures according to RTCM were used to calculate the discomfort degree-hours (temperatures outside of the range 20°C-26°C are considered as uncomfortable).

To assess the level of discomfort in a thermal zone, degree-hour DH is used and defined as the summation of the operative temperature degrees that are out of the range $[T_c-3^\circ\text{C}, T_c+3^\circ\text{C}]$ in summer conditions, and out of the range $[20^\circ\text{C}, 26^\circ\text{C}]$ for the rest of the year during a one-year simulation period (8760 hours), and it's calculated as follows:

$$DH = \sum_{i=1}^{8760} dH$$

$$dH = (T_{op,i} - (T_c + 3^\circ\text{C})) \cdot \Delta t \text{ when } T_{op,i} > T_c + 3^\circ\text{C in summer}$$

$$dH = ((T_c - 3^\circ\text{C}) - T_{op,i}) \cdot \Delta t \text{ when } T_{op,i} < T_c - 3^\circ\text{C in summer}$$

$$dH = (T_{op,i} - 26) \cdot \Delta t \text{ when } T_{op,i} > 26^\circ\text{C for the rest of the year}$$

$$dH = (20 - T_{op,i}) \cdot \Delta t \text{ when } T_{op,i} < 20^\circ\text{C for the rest of the year} \quad (2)$$

Where $T_{op,i}$ is the operative temperature at the center of the thermal zone, T_c is the comfort temperature calculated using the adaptive thermal comfort model as presented below, Δt is a one hour time period.

To carry out the optimization, the objective function was set to be an area-weighted mean discomfort degree-hours in multiple zones which is calculated as follows:

$$DDH_{mean} = \frac{A_{Z1} * DH_{Z1}(X) + A_{Z7} * DH_{Z7}(X) + A_{Z8} * DH_{Z8}(X) + A_{Z13} * DH_{Z13}(X)}{A_{Z1} + A_{Z7} + A_{Z8} + A_{Z13}} \quad (3)$$

Where A_{Zx} is the area of the thermal Zone Zx , DH_{Zx} is the discomfort degree-hours in the thermal zone Zx and $X = [x1, x2, x3, x4]$ is the vector of problem variables, which are $x1$: the overhangs projection in rooms 2-3, $x2$: the overhangs projection in the dining room, $x3$: the overhangs projection in rooms 5-6 and finally $x4$: the overhangs projection in the living room.

2.3 Thermal comfort model

An adaptive comfort model should be used, since the building is naturally ventilated and, on the other hand, occupants can adapt to the felt temperature to improve their comfort. Thereby, this section is dedicated to presenting such a model.

It should be noted that the thermal adaptive comfort model is only used for the calculation of the discomfort degree hours in summer conditions, in winter the calculation of discomfort degree hours is based on a constant temperature according to the Moroccan building thermal code (temperatures outside of the range 20°C-26°C are considered as uncomfortable).

According to standard EN 15251, an operative temperature T_{op} is considered as comfortable when it is between an upper and a lower limit defined according to the external running mean temperature T_{rm} in addition to the considered category of acceptability (categories I, II and III). For the EN 15251 standard, comfort temperature T_c has been calculated according to the following rules:

$$\left\{ \begin{array}{ll} T_{rm} < 10^{\circ}C & \text{Not applicable} \\ 10^{\circ}C < T_{rm} < 15^{\circ}C & \text{For the lower limits } T_c=23.75 \\ 10^{\circ}C < T_{rm} < 15^{\circ}C & \text{For the upper limits } T_c=0.33*T_{rm}+18.8 \\ 15^{\circ}C < T_{rm} < 30^{\circ}C & T_c=0.33*T_{rm}+18.8 \\ T_{rm} > 30^{\circ}C & \text{Not applicable} \end{array} \right. \quad (4)$$

Where T_{rm} , the external running mean temperature, is the weighted mean of the previous 7-day external air temperature, which is calculated using the relationship (5).

$$T_{rm} = \frac{(T_{ed-1}+0.8 T_{ed-2}+0.6 T_{ed-3}+0.5 T_{ed-4}+0.4 T_{ed-5}+0.3 T_{ed-6}+0.2 T_{ed-7})}{3.8} \quad (5)$$

Note that three acceptance limits (categories I, II and III) are defined by the following relationships (6)-(11).

$$\text{Category I upper limit : } T_{op} = T_c + 2^{\circ}C \quad (6)$$

$$\text{Category I lower limit : } T_{op} = T_c - 2^{\circ}C \quad (7)$$

$$\text{Category II upper limit : } T_{op} = T_c + 3^{\circ}C \quad (8)$$

$$\text{Category II lower limit : } T_{op} = T_c - 3^\circ\text{C} \quad (9)$$

$$\text{Category III upper limit : } T_{op} = T_c + 4^\circ\text{C} \quad (10)$$

$$\text{Category III lower limit : } T_{op} = T_c - 4^\circ\text{C} \quad (11)$$

It should be noted that, in this case, category II is considered to assess the thermal comfort of occupants, which corresponds to a normal expecting level and can be used for new buildings and renovations.

To assess the thermal comfort of occupants the only parameter that is taken into account is the operative temperature of the room. The “direct” effect of solar radiation through windows that hits the occupants is not accounted for, because we are not interested in that specific cases where inhabitants are close to the windows and hit directly by solar radiation.

2.4 Reference building

2.4.1 Building description

The studied building, a typical existing Moroccan house, is a two-storey multi-family building with two facades. Fig. 2, Fig. 3 and Fig. 4 present the 3D, 2D architectural plans of the house and its dimensions. Each floor has an area of 108 m² and a height of 2.7m. The ground floor consists of two bedrooms, a dining room, a garage, a WC, a bathroom, and a library as shown in Fig. 3. As for the first floor, it has a separated kitchen and a living room (see Fig. 4). It should be noted that each floor is occupied by four persons (two adults and two children).

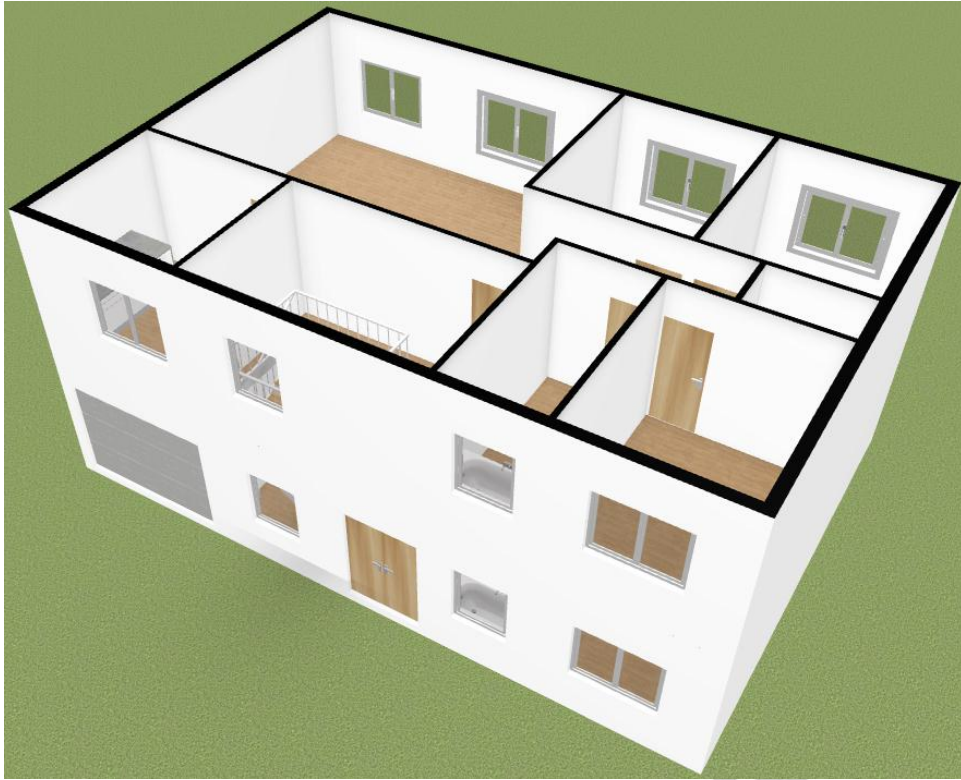


Fig. 2. 3D model of the building.

2.4.2 Composition of walls, ceiling and roof

The composition of walls, ceiling and roof for this house are summarized in Table 3. The thermophysical properties gathered are taken from measures from the BINAYATE software made by the AMEE, “Agence Marocaine pour l'Efficacité Energétique”, for several samples of these materials produced in Morocco which are close to the default values provided by TRNSYS [27].

In the GND floor, the average proportion of the glazing area is about 16.7%, its south facade has 21.2% of WWR (Window-to-Wall Ratio) and the north facades has a WWR of 12.3% due to the presence of the garage. In the other hand, the 1st floor has an average proportion of the glazed area of 19.4%, with a maximum of 21.2% and 17.6% for south and north facades, respectively.

Table 3 Composition of walls and thermophysical properties.

Construction element	Materials	Thickness (cm)	Thermal conductivity (W/m.K)	Thermal capacity (kJ/kg.K)	Density (kg/m ³)
<i>Exterior wall</i>	Cement	1.50	1.30	1.00	1900
	Hollow brick	20.00	0.21	0.74	664
<i>Ground floor</i>	Cement	1.50	1.30	1.00	1900
	Tile	2.00	1.30	0.84	2300
	Mortar	5.00	1.00	1.00	1700
	Heavy concrete	20.00	2.00	1.00	2450
	Gypsum plaster	1.00	0.56	1.00	1350
<i>Ceiling</i>	Hollow-core slab	16.00	1.04	1.00	1513
	Heavy concrete	7.00	2.00	1.00	2450
	Tile	2.00	1.30	0.84	2300
<i>Internal wall</i>	Cement	1.50	1.30	1.00	1900
	Hollow brick	10.00	0.19	0.74	918
	Cement	1.50	1.30	1.00	1900
<i>Glazing area</i>	Simple glazing	$U_{\text{value}}=5.74\text{W/m}^2.\text{K}$ and $g\text{-value}=0.87$			

2.4.3 Internal gains

For simulation to be as realistic as possible, internal gains were introduced into the simulation to account for occupant activities, lighting gains and equipment gains. These internal gains are from ISO 8996:2004 and ISO 07730:2005 [28,29] and are presented in Table 4.

Table 4 Internal gains.

	Type of gain	Daily schedule	Internal gains (W)
<i>Rooms 1 and 4</i>	- Lighting	- 20h to 22h	- 36 W
	- PC	- 20h to 22h	- 80 W
	- Laptop	- 20h to 22h	- 40 W
	- People	- 20h to 22h: 2 People doing sedentary activities during weekdays	- 126 W
<i>Rooms 2,3,5 and 6</i>	- Lighting	- 22h to 23h	- 36 W
	- People	- 22h to 23h: 2 People reclining	- 83 W
		- 23h to 7h: 2 People sleeping	- 72 W
<i>Dining room</i>	- Lighting	- 18h to 22h	- 72 W
	- People	- 07h to 8h, 12h to 14h and 18h to 20h: 4 people seating, 20h to 22h: 2 People (During WE: 7h to 22h 4 seating)	- 104 W

	- Kitchen	- 07h to 8h, 12h to 14h and 18h to 20h	- 500 W
	- Refrigerator	- 24h	- 300 W
	- TV	- 12h to 14h and 18h to 22 during week (During WE: 8h à 22h)	- 100 W
	- Lighting	- 18h to 22h	- 36 W
<i>Kitchen</i>	- Kitchen	- 07h to 8h, 12h to 14h and 18h to 20h	- 500 W
	- Refrigerator	- 24h	- 300 W
	- Washing machine	- 18h to 19h (2 days a week)	- 2000 W
	- Lighting	- 19h to 22h	- 72 W
<i>Living room</i>	- TV	- 12h to 14h and 18h to 22 during week (During WE: 8h to 22h)	- 100 W
	- People	- 07h to 8h, 12h to 14h and 18h to 20h: 4 people seating, 20h to 22h: 2 People (During WE: 7h to 22h 4 people seating)	- 104 W

2.4.4 Thermal zoning

The house is divided into 13 thermal zones. Rooms 2 and 3 are considered as a single zone because of the similarity of their geometries and internal gains, and so are rooms 5 and 6 of the 1st floor. As for the stairwell, it is modelled as a single zone with two nodes with a virtual-surface between them. The thermal zoning of the house is presented in Fig. 3 and Fig. 4.

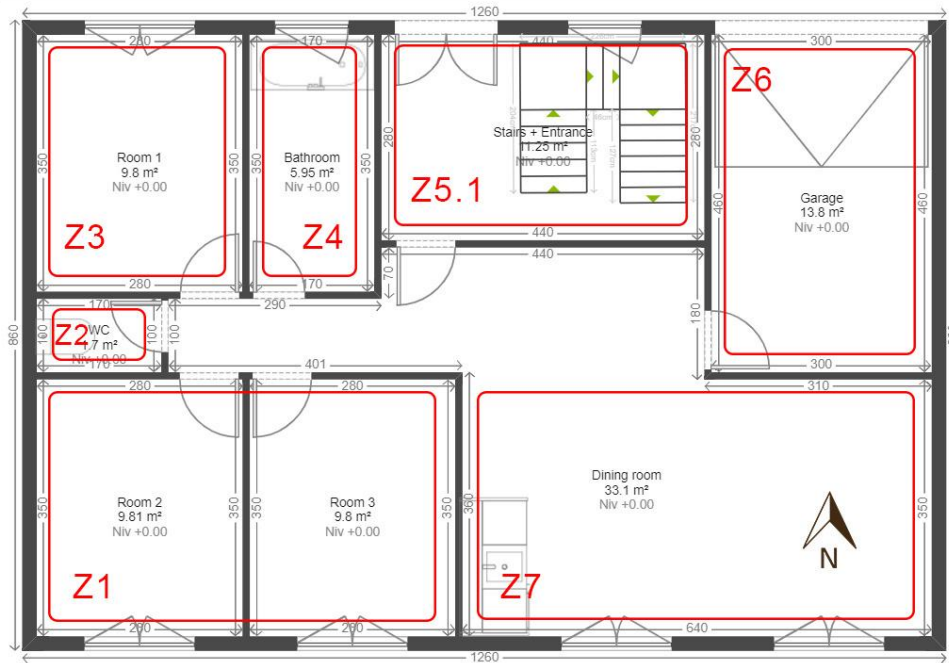


Fig. 3. Ground floor 2D plan and thermal zoning.

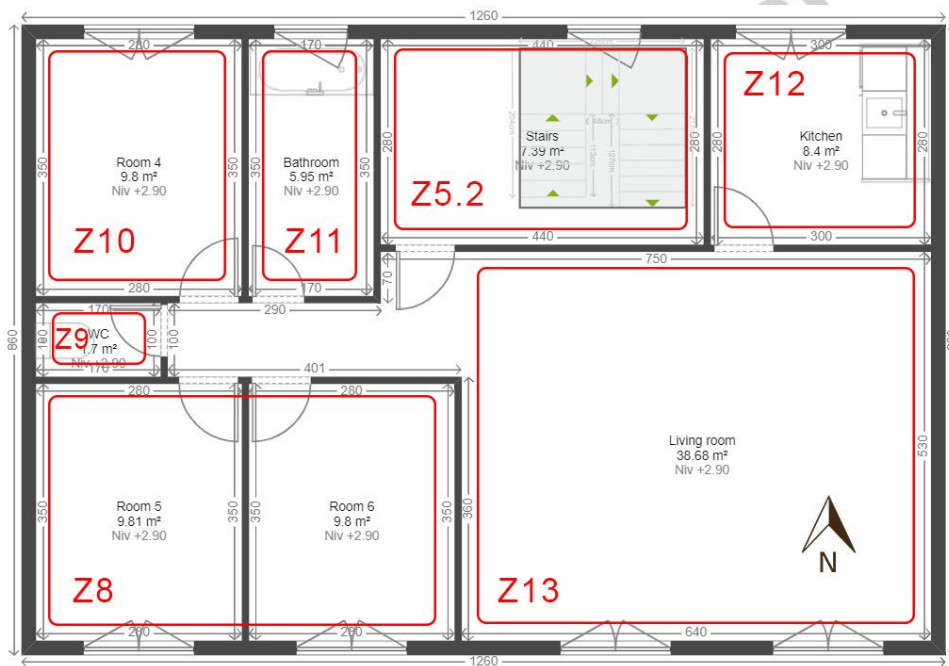


Fig. 4. 1st floor 2D plan and thermal zoning.

2.4.5 Locations and weather data

Typical meteorological Year (TMY) weather files were used in this study to describe these three cities climate characteristics, some of which are gathered in Table 5.

Table 5 Locations and weather data.

<i>Location</i>	Oujda (Morocco)	Marrakech (Morocco)	Casablanca (Morocco)
<i>Latitude</i>	34.8°N	31.6°N	33.6°N
<i>Longitude</i>	-1.9°E	-8.0°E	-7.7°E
<i>Elevation [m]</i>	470	466	55
<i>Highest average monthly temperature [°C]</i>	26.5 (July)	28.8 (July)	23.5 (August)
<i>Lowest average monthly temperature [°C]</i>	9.4 (January)	11.9 (January)	12.8 (January)
<i>Annual average solar global horizontal irradiance (GHI) [kWh.m⁻².day⁻¹]</i>	5.4	5.7	5.1
<i>Köppen climate classification</i>	BSk (cold semi-arid)	BSh (hot semi-arid)	Csa (Hot-summer Mediterranean)

2.5 Simulation assumptions

It is the TRNSYS transient system simulation tool that is adopted here to simulate the thermal behavior of the considered building that is modelled using type 56 (TRNBuild) and TRNSYS3D plug-in for SketchUp, which provides 3D capabilities.

Note that the following assumptions were adopted:

- 1- Each thermal zone was described by a unique airnode, except the stairwell which was described by two airnodes.
- 2- Windows are assumed to be closed permanently. And the natural ventilation and the air-coupling between zones and between zones and the exterior are not accounted for because the model would've been very time-consuming. So, we assumed that there is only an infiltration rate of 0.6 volume/h.
- 3- A time step of 1h was used.
- 4- The initial air temperature was set to 20°C and humidity to 50% in each zone.
- 5- The capacitance of each airnode was multiplied by a factor of 5 to account for furniture.
- 6- Solar absorptance of external walls and surfaces were set to 0.5.

7- Convective heat transfer coefficient for internal surfaces were calculated using internal calculation instead of a user-defined value, following the equation (12) [30].

$$h_{\text{inside}} = C(T_{\text{surf}} - T_{\text{air}})^a \quad (12)$$

where C and a are constants that depend on the surface type: ceiling, floor, vertical wall.

8- For external surfaces, the correlation (13) which takes into account the wind velocity (V) is used to calculate the convective heat transfer coefficient [31].

$$h_{\text{outside}} = 2.8 + 3.2V \quad (13)$$

9- TRNSYS Type77 is used to couple the building to the ground, which is based on the Kusuda correlation (14) [26].

$$T = T_{\text{mean}} - T_{\text{amp}} * \exp \left[-depth * \left(\frac{\pi}{365\alpha} \right)^{0.5} \right] * \cos \left\{ \frac{2\pi}{365} * \left[t_{\text{now}} - t_{\text{shift}} - \frac{depth}{2} * \left(\frac{365}{\pi\alpha} \right)^{0.5} \right] \right\} \quad (14)$$

3 Results and discussion

3.1 Reference building heat demand

Herein, the heating and cooling demands in zones 1, 7, 8 and 13 of the reference building (without overhangs) are presented. These 4 zones are particularly interesting because they are on the southern facade where overhangs will be both installed and optimized.

The heating and cooling demands presented in Table 6 are calculated using setpoints: 26 °C for cooling and 20 °C for heating.

Table 6 Annual heating and cooling demand in each zone for different climates.

	Dining room		Rooms 2-3		Rooms 5-6		Living room	
	Heating (kWh)	Cooling (kWh)	Heating (kWh)	Cooling (kWh)	Heating (kWh)	Cooling (kWh)	Heating (kWh)	Cooling (kWh)
<i>Casablanca</i>	825.0	961.8	1240.5	296.4	234.6	1502.2	311.1	2410.1
<i>Marrakech</i>	868.2	3372.1	1159.9	2116.8	199.0	2722.9	308.7	4136.1
<i>Oujda</i>	1245.7	2682.0	1610.0	1584.6	627.2	1683.0	889.7	2621.3

What is meant by "existing building" in this study is that the studied building represents the same characteristics as a building built before 2015 when the Moroccan building thermal code (RTCM) was not yet mandatory, it's not meant that it is a building that have been monitored. Unfortunately, there isn't monitoring data of this building to validate/calibrate our model. However, the energy performance (in kWh/m².year) of the building was compared with the reference values for residential buildings present in the Moroccan thermal code (Table 7 and Fig. 5), these data were extracted from RTCM documents [32] using WebPlotDigitizer [33], the values found by simulation are of the same order of magnitude.

Table 7 Comparison of the simulation results to the reference values according to RTCM.

	Casablanca	Marrakech	Oujda
<i>Heating (kWh)</i>	6394.9	6585.3	9938
<i>Cooling (kWh)</i>	7818	19250.5	13154.7
<i>Total energy demand (kWh)</i>	14212.9	25835.8	23092.7
<i>Total area (m²)</i>	202.2	202.2	202.2
<i>Energy performance of the building (kWh/m².year)</i>	70.3	127.8	114.2
<i>Energy performance according to RTCM (kWh/m².year)</i>	60	125	130

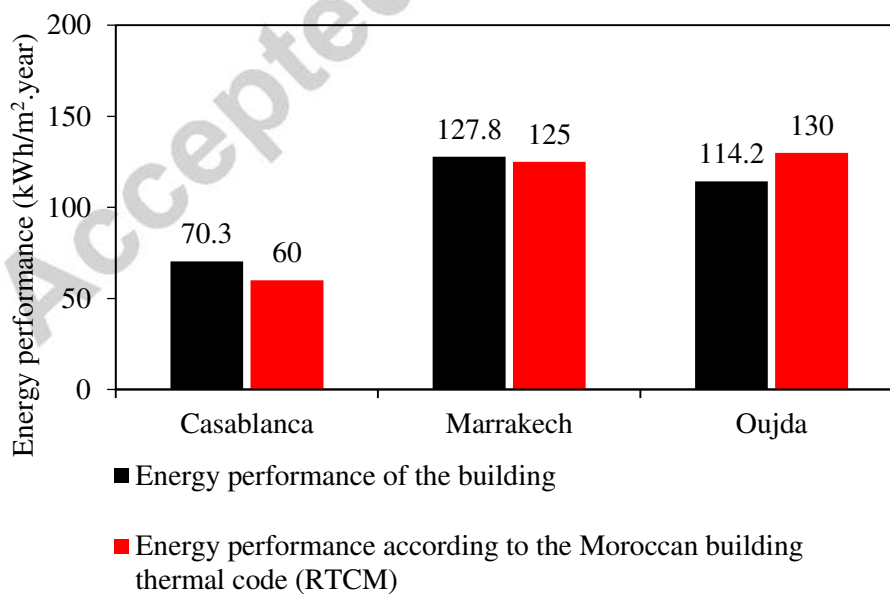


Fig. 5. Comparison of the simulation results to the reference values according to RTCM.

3.2 Optimized overhangs

Overhangs are usually used over a window to provide solar protection for the building. In this work, the eight windows of the south facade are equipped with overhangs optimized using a genetic algorithm. Fig. 6 shows the scatter plot of the optimization where area-weighted mean discomfort degree-hours is plotted as a function of discomfort degree-hours in rooms 2-3, it can be seen that the optimal solution (in red) leads to the minimal area-weighted mean discomfort degree-hours although it's not the point where discomfort degree-hours is minimal in thermal zone 1.

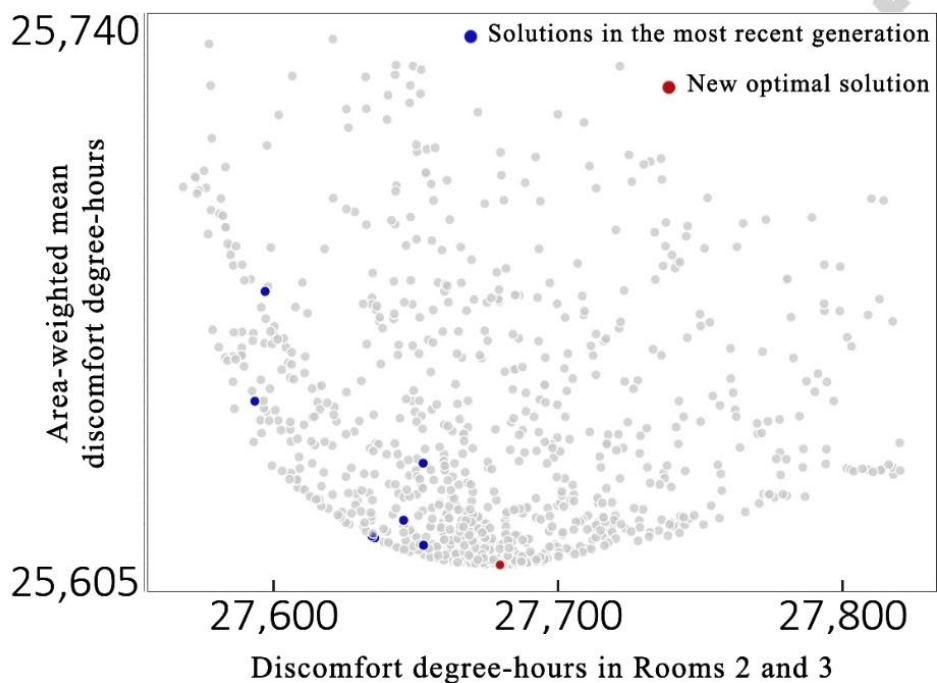


Fig. 6. Optimization scatter plot.

In order to optimize the overhangs' projection, some combinations of overhang's depths (four parameters, each one for one of the four thermal zones facing south) have been considered for the genetic algorithm that varies from place to place with a step of 1cm. In order to narrow the search space, a less accurate optimization has been performed upstream using a 3cm step when defining parameters in jEPlus, that's how we got an approximate solution thus helping to specify a maximum value for each overhang depth (Table 8), this

maximum value is the upper limit of the domain of definition where the depth parameter will vary.

Table 8 Optimization results.

		Thermal zones			
		Z1	Z7	Z8	Z13
<i>Casablanca</i>	Overhang projection values (m)	0.00 to 0.11	0.00 to 0.21	0.00 to 0.26	0.00 to 0.41
	Optimal value (m)	0.00	0.07	0.21	0.36
<i>Marrakesh</i>	Overhang projection values (m)	0.00 to 0.21	0.00 to 0.41	0.00 to 0.31	0.00 to 0.41
	Optimal value (m)	0.00	0.19	0.24	0.32
<i>Oujda</i>	Overhang projection values (m)	0.00 to 0.16	0.00 to 0.31	0.00 to 0.26	0.00 to 0.31
	Optimal value (m)	0.00	0.22	0.18	0.24

It should be noted that thermal zone 1 which includes rooms 2 and 3 does not require overhangs, which could be explained by the low need for cooling in these rooms. It will also be noted that zone 13 which represents the living room has the largest sizes of overhangs.

3.3 Impact on energy demand

The following figures are showing that overhangs reduce the need for air conditioning while slightly increasing heating requirements. On the other hand, heating and cooling demands remain practically unchanged in rooms 2 and 3 since there are no overhangs.

3.3.1 Casablanca city

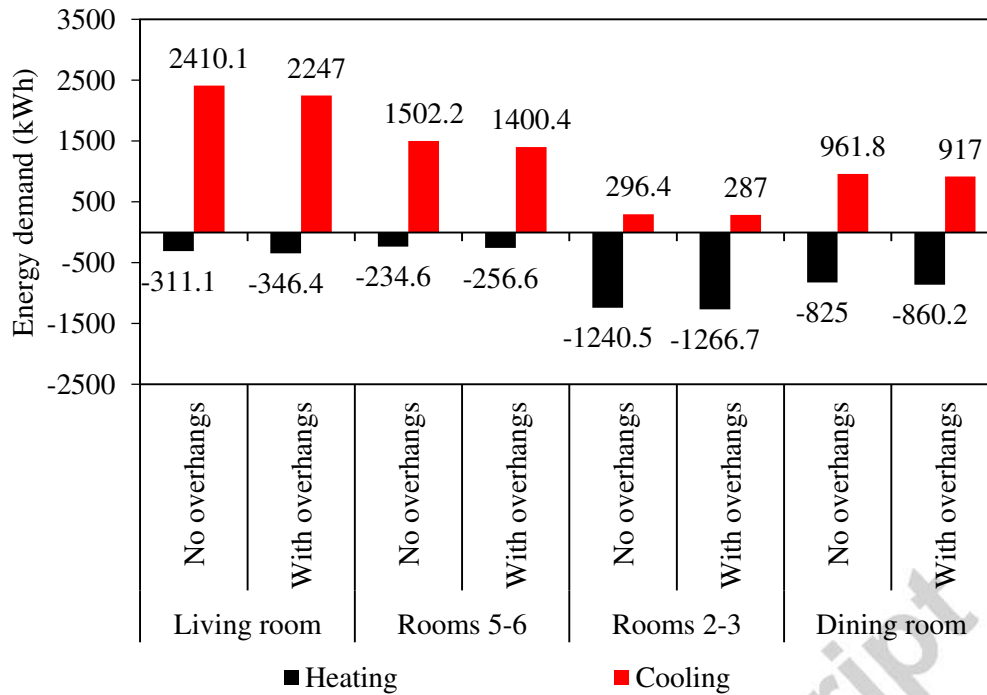


Fig. 7. Cooling (+) and heating (-) demands of the building [kWh].

For the climate of Casablanca city, the results show a decrease in the cooling demand of 6.8% and an increase in the heating demand of 11.3% in the living room. In the dining room, there is a decrease of 4.7% in the cooling demand and an increase of 4.2% in the heating demand. Also, the cooling demand decreases by 6.8% and the heating demand increases by 9.4% in rooms 5 and 6. However, there are no significant changes in cooling and heating demand for rooms 2 and 3 between the optimal case with overhangs and the reference case without overhangs (see Fig. 7).

Alternatively, there is a total decrease in demand for cooling of 319.1kWh and an increase in the heating demand of 118.7kWh.

3.3.2 Marrakech city

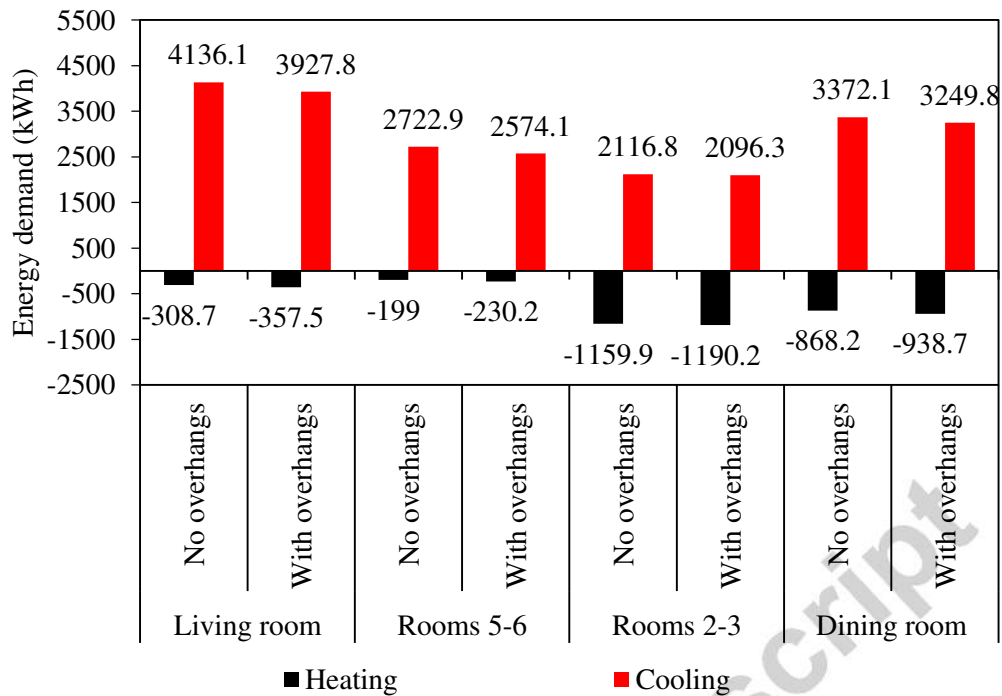


Fig. 8. Cooling (+) and heating (-) demands of the building [kWh].

For the climate of Marrakech city, a decrease in the cooling demand of 5% and an increase in the heating demand of 15.8% is shown in the living room. Furthermore, in the dining room, there is a decrease of 3.6% in the cooling demand and an increase of 8.1% in the heating demand. In addition, the cooling demand decreases by 5.5% and the heating demand increases by 15.7% in rooms 5 and 6, while there are no significant changes in cooling and heating demand for rooms 2 and 3 between the optimal case with overhangs and the reference case without overhangs as shown in Fig. 8.

Alternatively, there is a total decrease in demand for cooling of 499.9kWh and an increase in the heating demand of 180.8kWh.

3.3.3 Oujda city

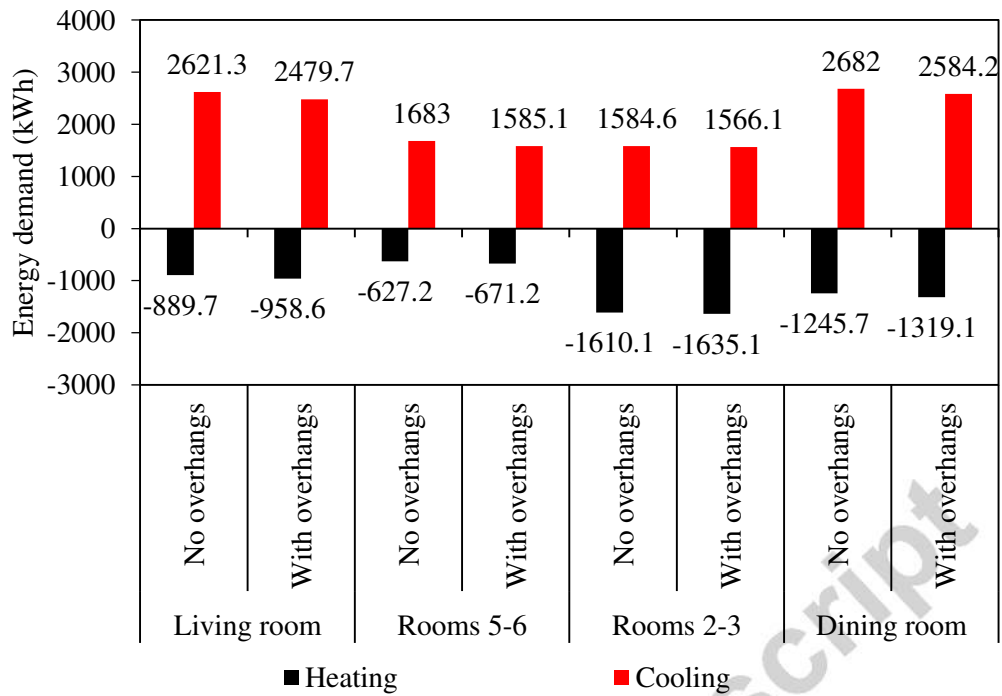


Fig. 9 Cooling (+) and heating (-) demands of the building [kWh].

For the climate of Oujda city, a decrease in the cooling demand of 5.4% and an increase in the heating demand of 7.7% is found in the living room. In addition, the dining room shows a decrease of 3.6% in the cooling demand and an increase of 5.9% in the heating demand. Also, the cooling demand decreases by 5.8% and the heating demand increases by 7% in rooms 5 and 6, while there are no significant changes in cooling and heating demand for rooms 2 and 3 between the optimal case with overhangs and the reference case without overhangs as shown in Fig. 9.

Alternatively, there is a total decrease in demand for cooling of 355.8kWh and an increase in the heating demand of 211.3kWh.

3.4 Impact on comfort

The optimization was aimed at minimizing the discomfort degree-hours, which improves the occupant's comfort. Figs. 10, 11 and 12 show the discomfort felt by the occupants as a percentage of hours of discomfort over a whole year, calculated using the relationship (15).

$$\%discomfort = \frac{\text{Hours of discomfort}}{8760} * 100 \quad (15)$$

In this study, we chose to use the hours of discomfort based on an adaptive comfort model for summer conditions, and constant temperatures for the rest of the year according to RTCM instead of PPD to evaluate comfort, since the building does not have HVAC facilities and is assumed to be naturally ventilated.

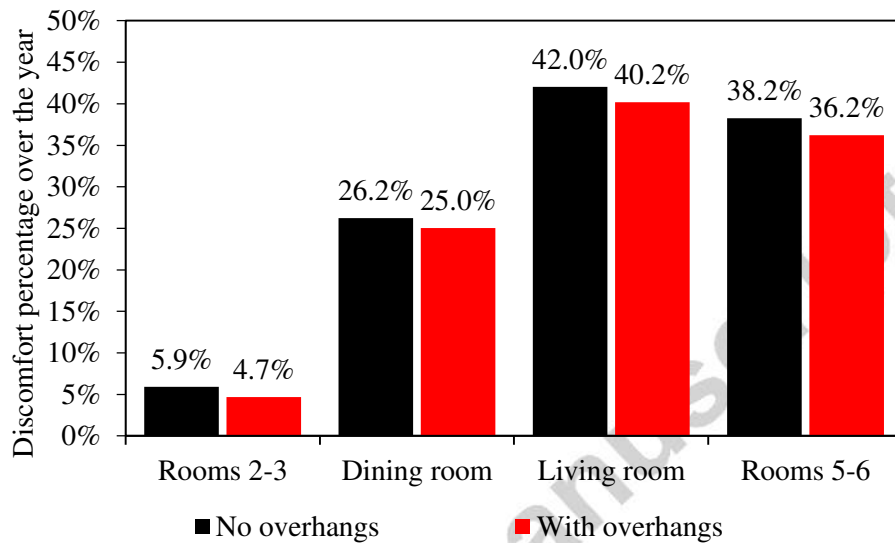


Fig. 10. Impact of optimal solution on comfort for Casablanca climate.

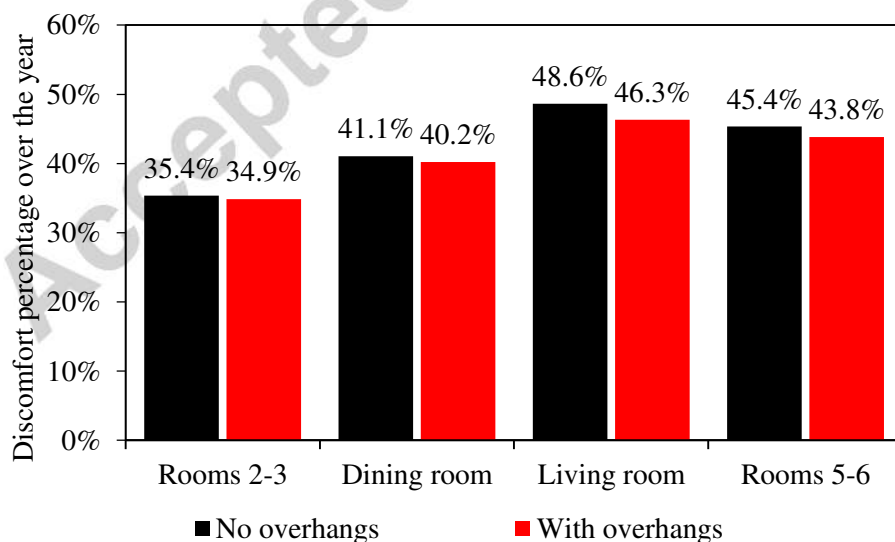


Fig. 11. Impact of optimal solution on comfort for Marrakesh climate.

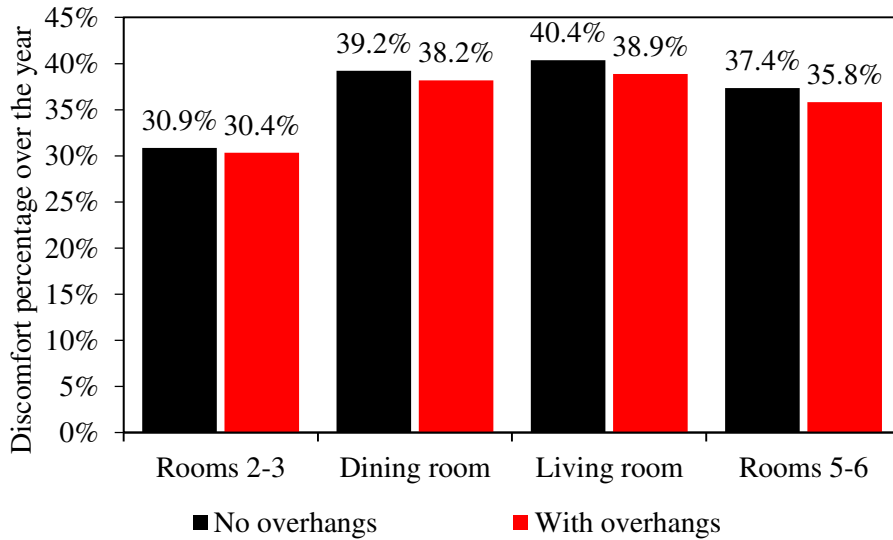


Fig. 12. Impact of optimal solution on comfort for Oujda climate.

For the three climates, the occupants' comfort is improved in all four zones of the building that are facing south.

The reduction in discomfort hours is not very significant because the use of overhangs is not sufficient to prevent the overheating of the building, other passive techniques such as movable shadings, natural ventilation, cool painting and insulation have to be used in order to get a better discomfort reduction in the building.

3.5 Comparison of the three different climates

Table 9 Energy savings.

	Casablanca	Marrakech	Oujda
<i>Heating (kWh)</i>	6394.9	6585.3	9938
<i>Cooling (kWh)</i>	7818	19250.5	13154.7
<i>Heating demand increase (kWh)</i>	118.7 (+1.9%)	180.8 (+2.8%)	211.3 (+2.1%)
<i>Cooling savings (kWh)</i>	319.1 (-4.1%)	499.9 (-2.6%)	355.8 (-2.7%)

The impact of overhangs on the energy savings in the building for the three climates can be ranked as follows: Casablanca first with 4.1% savings in cooling while heating demand only increases by 1.9%, followed by Oujda where the optimization achieves 2.7% savings in

cooling and 2.1% increase in heating demand, Marrakech ranks last with an impact on heating demand (2.8%) greater than the energy savings in cooling (2.6%) as shown in Table 9.

Table 10 Decrease in discomfort hours.

	Casablanca	Marrakech	Oujda
<i>Decrease in discomfort hours in Rooms 2-3</i>	107.8	43.8	45.6
<i>Decrease in discomfort hours in Dining room</i>	105.1	73.6	91.1
<i>Decrease in discomfort hours in Living room</i>	162.9	200.6	130.5
<i>Decrease in discomfort hours in Rooms 5-6</i>	176.1	132.3	134
<i>Area weighted mean discomfort hours reduction</i>	138.3	123	104.4

Regarding the impact on comfort, the optimized overhangs are more efficient in Casablanca climate where they reduced the area weighted mean discomfort hours by 138.3 hours in a year, followed by Marrakech with 123 discomfort hours decreased, and finally Oujda with 104.4 hours as shown in Table 10.

4 Conclusions

In this study, we proposed a methodology where the coupling between a GA optimization tool and a building energy simulation program is done. The methodology is then applied to a simple case focusing on improving the occupants' thermal comfort in an existing Moroccan residential building. To this end, we sought to prevent overheating of the building through the installation of shading devices, which are one of the best techniques to limit the overheating of the building caused by solar heat gains through the transparent envelope of the building.

Initially, the building was modelled taking into account the internal gains and behavior of occupants that are one of the major causes of overheating in summer. Then, a simulation of the reference building was made in order to get the comfort indices (hours of discomfort and

percentage of hours of discomfort) and the thermal performances (heating and cooling demands) of the existing building before any change to improve it.

Throughout the study, the comfort of the occupants in summer conditions is evaluated through an adaptive comfort model (EN 15251), for the rest of the year, constant values of temperature were used to assess the thermal comfort according to RTCM values (temperatures outside of the range 20°C-26°C are considered as uncomfortable). Overhangs were optimized for the south facade of the building in three different climates (hot semi-arid, cold semi-arid and hot-summer Mediterranean climates) taking into account the needs of each thermal zone regarding comfort. The optimization was performed with a genetic algorithm (NSGA-II) thanks to the coupling of jEPlus and TRNSYS, the data used as an objective are the discomfort degree-hours. The optimum values thereby obtained were used for overhangs dimensions.

After having dimensioned the overhangs, the optimized building was compared to the benchmark case. The findings are quite convincing. Thus, a 499.9kWh (2.7%) cooling demand reduction is observed for the Marrakech climate, with an increase in the heating demand of 180.8kWh (2.8%). At the same time, these values are 355.8kWh (2.7%) and 211.3kWh (2.1%) for Oujda, and 319.1kWh (4.1%) and 118.7kWh (1.9%) for Casablanca.

The thermal comfort of the occupants has been enhanced. Indeed, the reduction of the percentage of discomfort is achieved in each zone of the south facade of the building. As a result, the thermal comfort of the occupants is improved in conjunction with the thermal performance of the building.

It would be interesting as a future work to perform a multi-objective optimization with more decision variables such as insulation thickness, glazing type, different heating and cooling setpoints, width and height of the windows, orientation of the building, ...etc.

Acknowledgement

The authors would like to thank the “National Center for Scientific and Technical Research” for funding this work through the PPR project “Promotion of solar energy and energy efficiency in the oriental region of Morocco”.

Declaration of interest

The authors declare no potential conflicts of interest regarding authorship and/or publication of this article.

References

- [1] AMEE, Règlement thermique de construction au Maroc (RTCM), (2013).
- [2] G. Yun, K.C. Yoon, K.S. Kim, The influence of shading control strategies on the visual comfort and energy demand of office buildings, *Energy Build.* 84 (2014) 70–85. doi:10.1016/j.enbuild.2014.07.040.
- [3] G. Kim, H.S. Lim, T.S. Lim, L. Schaefer, J.T. Kim, Comparative advantage of an exterior shading device in thermal performance for residential buildings, *Energy Build.* 46 (2012) 105–111. doi:10.1016/j.enbuild.2011.10.040.
- [4] L. Bellia, F. De Falco, F. Minichiello, Effects of solar shading devices on energy requirements of standalone office buildings for Italian climates, *Appl. Therm. Eng.* 54 (2013) 190–201. doi:10.1016/j.applthermaleng.2013.01.039.
- [5] P. Samani, V. Leal, A. Mendes, N. Correia, Comparison of passive cooling techniques in improving thermal comfort of occupants of a pre-fabricated building, *Energy Build.* 120 (2016) 30–44. doi:10.1016/j.enbuild.2016.03.055.
- [6] A. Ebrahimpour, M. Maerefat, Application of advanced glazing and overhangs in residential buildings, *Energy Convers. Manag.* 52 (2011) 212–219. doi:10.1016/j.enconman.2010.06.061.

- [7] A. Aldawoud, Conventional fixed shading devices in comparison to an electrochromic glazing system in hot, dry climate, *Energy Build.* 59 (2013) 104–110. doi:10.1016/j.enbuild.2012.12.031.
- [8] L. Olivieri, E. Caamaño-Martín, F.J. Moralejo-Vázquez, N. Martín-Chivelet, F. Olivieri, F.J. Neila-Gonzalez, Energy saving potential of semi-transparent photovoltaic elements for building integration, *Energy.* 76 (2014) 572–583. doi:10.1016/j.energy.2014.08.054.
- [9] C. Cornaro, G. Basciano, V. Puggioni, M. Pierro, Energy Saving Assessment of Semi-Transparent Photovoltaic Modules Integrated into NZEB, *Buildings.* 7 (2017) 9. doi:10.3390/buildings7010009.
- [10] F. Frasca, M. Lovati, C. Cornaro, D. Moser, A. Siani, Use of photovoltaic modules as static solar shadings: Retrofit of a paleontological site in Rome., in: 2017.
- [11] P. Penna, A. Prada, F. Cappelletti, A. Gasparella, Multi-objectives optimization of Energy Efficiency Measures in existing buildings, *Energy Build.* 95 (2015) 57–69. doi:10.1016/j.enbuild.2014.11.003.
- [12] E. Asadi, M.G. da Silva, C.H. Antunes, L. Dias, L. Glicksman, Multi-objective optimization for building retrofit: A model using genetic algorithm and artificial neural network and an application, *Energy Build.* 81 (2014) 444–456. doi:10.1016/j.enbuild.2014.06.009.
- [13] L. Magnier, F. Haghghat, Multiobjective optimization of building design using TRNSYS simulations, genetic algorithm, and Artificial Neural Network, *Build. Environ.* 45 (2010) 739–746. doi:10.1016/j.buildenv.2009.08.016.
- [14] M. Hamdy, A. Hasan, K. Siren, Applying a multi-objective optimization approach for Design of low-emission cost-effective dwellings, *Build. Environ.* 46 (2011) 109–123. doi:10.1016/j.buildenv.2010.07.006.

- [15] F. Roberti, U.F. Oberegger, E. Lucchi, A. Troi, Energy retrofit and conservation of a historic building using multi-objective optimization and an analytic hierarchy process, *Energy Build.* 138 (2017) 1–10. doi:10.1016/j.enbuild.2016.12.028.
- [16] N. Delgarm, B. Sajadi, S. Delgarm, F. Kowsary, A novel approach for the simulation-based optimization of the buildings energy consumption using NSGA-II: Case study in Iran, *Energy Build.* 127 (2016) 552–560. doi:10.1016/j.enbuild.2016.05.052.
- [17] B.J. Futrell, E.C. Ozelkan, D. Brentrup, Bi-objective optimization of building enclosure design for thermal and lighting performance, *Build. Environ.* 92 (2015) 591–602. doi:10.1016/j.buildenv.2015.03.039.
- [18] X. Chen, H. Yang, W. Zhang, Simulation-based approach to optimize passively designed buildings: A case study on a typical architectural form in hot and humid climates, *Renew. Sustain. Energy Rev.* (2017). doi:10.1016/j.rser.2017.06.018.
- [19] Z.C. Tian, W.Q. Chen, P. Tang, J.G. Wang, X. Shi, Building Energy Optimization Tools and Their Applicability in Architectural Conceptual Design Stage, *Energy Procedia.* 78 (2015) 2572–2577. doi:10.1016/j.egypro.2015.11.288.
- [20] C. Christensen, R. Anderson, S. Horowitz, A. Courtney, J. Spencer, BEopt™ Software for Building Energy Optimization: Features and Capabilities., (2006).
- [21] Y. Zhang, Use jEPlus as an efficient building design optimisation tool, in: CIBSE ASHRAE Tech. Symp. Imp. Coll. Lond. UK – 18th 19th April 2012, 2012.
- [22] M. Palonen, M. Hamdy, A. Hasan, MOBO a new software for multi-objective building performance optimization, in: BS2013, France, 2013.
- [23] L. Caldas, GENE_ARCH: An Evolution-Based Generative Design System for Sustainable Architecture, in: *Intell. Comput. Eng. Archit.*, Springer, Berlin, Heidelberg, 2006: pp. 109–118. doi:10.1007/11888598_12.

- [24] F.P. Chantrelle, H. Lahmidi, W. Keilholz, M.E. Mankibi, P. Michel, Development of a multicriteria tool for optimizing the renovation of buildings, *Appl. Energy*. 88 (2011) 1386–1394. doi:10.1016/j.apenergy.2010.10.002.
- [25] M. Wetter, GenOpt®-A Generic Optimization Program., in: Rio de Janeiro, 2001.
- [26] Y. Zhang, I. Korolija, Performing complex parametric simulations with jEPlus, in: 2010.
- [27] S.A. Klein, J.A. Duffie, W.A. Beckman, TRNSYS - A Transient Simulation Program., *ASHRAE Trans.* 82 (1976) 623–633.
- [28] ISO 8996:2004 Ergonomics of the thermal environment -- Determination of metabolic rate, (2004).
- [29] BS EN ISO 07730:2005 Ergonomics of the thermal environment -- Analytical determination and interpretation of thermal comfort using calculation of the PMV and PPD indices and local thermal comfort criteria, (2005).
- [30] TRNSYS 17, Multizone building (Type56 - TRNBuild), 2012.
- [31] S. Soutullo, R. Enriquez, C. San Juan, J.A. Ferrer, M.R. Heras, Energy balances of four office buildings in different locations in Spain, *Proceedings of the IBPSA-Canada's Biennial Conference in Winnipeg, Manitoba (Canada) (n.d.)* 19–22.
- [32] AMEE, Publications, (n.d.).
http://www.amee.ma/index.php?option=com_content&view=article&id=492&Itemid=873&lang=fr (accessed March 14, 2018).
- [33] A. Rohatgi, WebPlotDigitizer - Extract data from plots, images, and maps (Version 4), (2017). <https://automeris.io/WebPlotDigitizer/> (accessed March 14, 2018).

HIGHLIGHTS

- Building energy simulation coupled to a genetic algorithm optimization.
- Overhangs optimization via an NSGA-II algorithm.
- Optimized overhangs reduce the cooling demand by 4.1% for Casablanca climate.
- Thermal comfort and thermal performance improvements show no contradiction.

Accepted manuscript